Egyptian Journal of Radiology and Nuclear Medicine

RESEARCH

Open Access

Magnetic resonance imaging correlation with molecular and epigenetic markers in assessment of breast cancer

Aya S. El-Rawy[1*], Hoda Y. Abdallah[2], Marwa A. Suliman[3], Mohamed R. Habba[1] and Azza A. Gad[1]

Abstract

Background: Breast cancer is a heterogeneous disease with a wide range of clinical behavior, histologic subtypes, therapeutic options, and outcomes. The different biology and histology of breast cancer display different tumor morphology at breast magnetic resonance imaging (MRI). However, few studies have examined the relationship between the MRI morphological, kinetic features and molecular and epigenetic markers in breast cancer assessment. The study aimed to evaluate the correlation between MRI morphological and kinetic features, molecular and an epigenetic marker (linc-ITGB1) in breast cancer cases. A total of 115 women (80 cases and 35 controls) with BIRAD 4 category breast lesions were included. The association between the MRI morphological & kinetic features, apparent diffusion coefficient (ADC) values, and molecular and the epigenetic marker (linc-ITGB1) was evaluated using Mann–Whitney and Chi-square tests.

Results: The shape ($p=0.009$), size of the lesion ($p=0.003$), and pattern of enhancement ($p\leq0.001$) were significantly correlated with the molecular markers. Luminal subtypes are more likely to be presented with irregular shaped and non-circumscribed margin masses (97% for luminal A and 94.1% for luminal B). Triple-negative cancers are frequently presented with regular masses, circumscribed margins, and peripheral rim enhancement (50% of TN tumors). HER2-positive cancers are more likely to be multifocal/multicentric and are more associated with non-mass pattern of enhancement as compared to HER2-negative cancers. Perilesional edema was also significantly correlated with HER2-positive lesions ($p=0.009$). Although the epigenetic marker linc-ITGB1 was overexpressed by 4.85-folds in breast cancer cases compared to benign controls, we could not find any significant correlation between its expression level and the MRI features or molecular subtypes ($p=0.948$).

Conclusions: MRI features can be a reliable predictor of breast cancer molecular subtypes. The epigenetic marker linc-ITGB1 has a potential role in breast cancer pathogenesis but with no significant correlation with either the MRI features or molecular subtypes of the lesions.

Keywords: Breast cancer, MRI, Molecular subtypes, Epigenetics, LncRNAs, Linc-ITGB1

Background

Breast cancer (BC) is a heterogeneous disease with various intrinsic molecular subtypes that differ in clinical outcomes and treatment responses as well as prognosis [1, 2]. The different biology and histology of BC display different tumor morphologies at breast magnetic resonance imaging (MRI) [3].

Over the last years, several treatments such as chemotherapy, radiation and hormone therapy have significantly

*Correspondence: Ayarawy88@gmail.com; Aya_alrawy@med.suez.edu.eg

[1] Department of Radiology, Faculty of Medicine, Suez Canal University, Ismailia, Egypt
Full list of author information is available at the end of the article

reduced the mortality of BC patients. However, the prognosis of the patients with distal metastasis remained poor [4]. The complicated molecular mechanisms in BC pathogenesis remain largely vague despite the advancement in pathogenesis of BC. Thus, new biomarkers are needed to improve the detection and prognostic outcome of BC [5].

There are five main intrinsic or molecular subtypes of BC that are based on the genes the cancer expresses [3]: estrogen receptor (ER), progesterone receptor (PR), human epidermal growth factor receptor 2 (HER2), and Ki67. They are considered the most widely used markers for defining BC molecular subtypes [2, 3, 6].

Increasing studies indicated that epigenetics plays an important role in cancer. The long non-coding RNA (lncRNA), a type of non-coding RNA that is considered as a major epigenetic alteration, plays an important role in cancer progression. So, lncRNAs have been lately considered as potential biomarker and therapeutic targets [6, 7]. One of the well-known lncRNAs is linc-ITGB1 that was reported to promote cell proliferation and metastasis in breast tumorigenesis and may represent a valuable independent prognostic indicator for BC [5].

Magnetic resonance imaging (MRI), a noninvasive and highly sensitive examination, has been increasingly used in the assessment of breast disease, including the differential diagnosis of benign and malignant lesions, preoperative evaluation, pretreatment planning and efficacy prediction [8].

In many studies, the correlation between the MRI morphology and the molecular subtypes of breast cancer has been reported. However, few studies have examined the quantitative relationship between the MRI morphological features, molecular markers and epigenetic markers in breast cancer assessment [1, 9].

The purpose of this study was to investigate the correlation between the morphological and kinetic features of breast MRI, molecular and the epigenetic marker in breast cancer assessment, which may allow prediction of the behavior of the disease, suggesting new types of disease classification and ultimately establishing an earlier diagnosis and thereby treatment for BC patients.

Methods

Target population

Eighty patients with unilateral or bilateral suspicious breast lesions (BIRADS 4 or more) were detected by any imaging modality (mammography or breast ultrasound) in Suez Canal University Hospital and Oncology Hospital from April 2020 to September 2021. We included all female patients with suspicious breast mass (BIRADS 4 or more) but our exclusion criteria encompassed psychotic patients, pregnant and patients with benign breast masses, patients with incomplete information on ER, PR, and HER2 status, patients with insufficient biopsy specimen, general contraindications to breast biopsy, and absolute contraindication to MRI.

Data collection

According to our study expected outcomes, we had four groups of data variables that were obtained for each patient upon referral. This was encompassing: clinical data revealed from history and examination, MRI scan data results, molecular data results and epigenetic analysis data results.

MRI scan

It was done at the MRI-Unit, Suez Canal University Hospital, Diagnostic Radiology Department, Ismailia. The procedure was done using 1.5 Tesla MR scanner (Philips Medical Systems, Achieva 1.5T A-series). Patient was transferred to the MRI unit where bilateral breast MRI was performed. The MRI protocol was done using breast surface coil with the patient in the prone position. The study was performed in the second week of the menstrual cycle for premenopausal women to minimize the amount of background parenchymal enhancement [10]. The imaging acquisition protocol used a localizer and non-contrast-enhanced (pre-contrast) sequences/series as follows: axial T1-weighted turbo spin echo (TR/TE = 500/5.3 ms) [10], sagittal and axial T2-weighted images using turbo spin echo (TR/TE = 120/4.9 ms) [10], axial short-time inversion recovery (STIR) (TR/TE = 80/6.5 ms), and a pre-contrast fat-saturated T2-weighted pulse sequence to separate cysts from solid masses [8]. The diffusion-weighted imaging (DWI) sequences included single-shot echo planar sequence: TR/TE: 5000/110 ms, FOV: 320 mm, matrix: 128 × 128, slice thickness: 3.5-mm, 0.7-mm slice gap, b values: 0–1000 s/mm^2 [11]. The ADC measurement was taken using manual placed multiple ROIs; cystic or necrotic portions of the tumor were avoided [12]. Contrast-enhanced sequences/series was done using a bolus of contrast (gadolinium-diethylene tri aminopenta-acetic acid; Gd-DTPA) (Magnevist, Schering AG Berlin, Germany) injected manually intravenous at a dose of 0.1 mmol per kilogram body weight (0.1 mmol/kg) followed by saline flush [3]. Six dynamic acquisitions were taken: one before and five after intravenous injection of contrast material, using the volume-interpolated GRE sequence (T1High Resolution Isotropic Volumetric Examination) with the parameters (TR/TE = 2.8/9 ms) and slice thickness = 1.5 mm [10]. Finally, post-processing included subtraction, maximum intensity projection (MIP), and creating time/signal intensity curve by placing the region of interest (ROI) at the most enhanced part within the

lesion. The findings were evaluated in accordance with the American College of Radiology Breast Imaging-Reporting and Data System (ACR BI-RADS) 5th edition Lexicon (2013).

Molecular evaluation

All tissue samples were fixed with 10% formalin and embedded in paraffin blocks. Tissue sections were stained with by hematoxylin and eosin (H&E). Additional sections were used for immunohistochemical (IHC) staining. All histopathological and IHC-stained slides were reviewed by two independent pathologists. Immunohistochemical staining and evaluation: Formalin-fixed paraffin-embedded specimens were cut into 4-µm sections and mounted on MAS-GP-coated slides (Matunami Glass Ind., Osaka, Japan) [4]. After de-paraffinization, sections were heated with an autoclave in 0.1 mM-EDTA Tris/H CL buffer (pH 9.0) for 1 h at 121 °C for antigen retrieval. Then, the sections were incubated with 0.3% H2O2 in absolute methanol for 30 min and then incubated with Protein Block Serum Free Reagent (Dako) for 15 min [4]. The sections were incubated with primary antibodies, at 4 °C overnight. This was followed by sequential 60-min incubations with secondary antibodies (Envision + System-HRP Labelled Polymer, Dako) and visualization with the Liquid DAB Substrate Chromogen System (Dako). All slides were lightly counterstained with hematoxylin for 30 s prior to dehydration and mounting [3, 4].

Epigenetic analysis

Expression profiling of Linc-ITGB1 from either FFPE tissue sections or frozen tissues was performed following the protocols supplied by the manufacturer and assessed via the following steps: RNA extraction and quality assessment, reverse transcription, gene expression analysis using quantitative real-time (qRT-PCR), and data analysis.

Statistical analysis

Tumor MRI morphological and dynamic features were assessed by two radiologists. Data were fed to the computer and analyzed using IBM SPSS software package version 20.0.

Ethical considerations

An informed written consent was taken from all the participants before taking any data or doing any investigations or imaging techniques and manuscript publication as well. No identifying images or clinical details of participants have been disclosed in the research.

Results

The study encountered one hundred and fifteen patients: eighty cases with pathologically proven breast cancer and thirty-five controls (for relative gene expression assessment). Most of the patients were above 50 years old with mean age of 52.85 ± 8.87 and were postmenopausal (57.5%). 91.3% of the patients were symptomatic and 77.5% of them are multiparous. All of cases underwent breast biopsy and pathological, immunohistochemical, epigenetic marker (Linc-ITGB1 gene) assessment as well as dynamic MRI study with assessment of T2WIs signal intensity of the lesion, evaluation of the shape, margin, pattern of enhancement, ADC values and lymph node involvement.

Regarding the pathological assessment, most of the cases were IDC-NOS and few cases of ILC and only one case of mucinous mammary adenocarcinoma. Luminal A subtype was the most common type in this study diagnosed in 46.3% of cases followed by luminal B HER2 − ve subtype in 23.8% and luminal B HER2 +ve subtype in 15% of cases. Triple-negative subtype is diagnosed in 10% of the cases and only 5% of the cases diagnosed with HER 2-amplified subtypes (Fig.1).

In MRI assessment, lesions were single in 55% of cases, multifocal in 28.8% and multicentric in 16.3% of cases. According to the type of enhancement, mass enhancement was found in 78.8% of the cases, non-mass

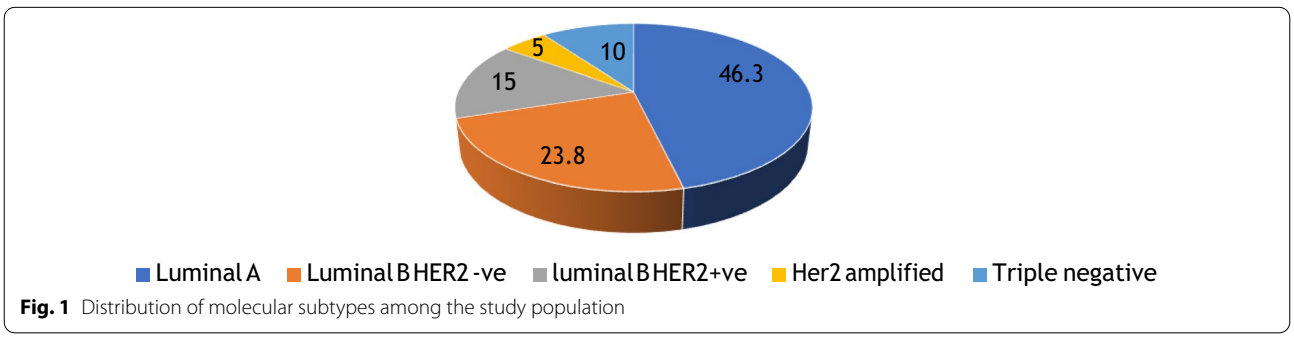

Fig. 1 Distribution of molecular subtypes among the study population

enhancement in 11.3% of cases and mass with non-mass enhancement in 10% of cases. Most of the lesions were more than 2 cm. Irregular shape, spiculated margin and low-to-intermediate T2WIs signal intensity with heterogeneous internal enhancement were seen in most of the cases (Table 1, Fig.2). Most of the cases of non-mass enhancement showed segmental distribution and clumped pattern of enhancement. All the lesions of non-mass pattern of enhancement showed low-to-intermediate signal in T2 WIs.

Assessment of the signal-intensity curve revealed that 62.5% of the lesions showed washout curve of enhancement and 37.5% showed plateau curve. Most of the cases (80%) showed suspicious axillary lymph nodes. The mean ADC values were 0.96 ± 0.05. 60% of the cases. Associated features were mainly perilesional edema and skin thickening. Nipple invasion and pectoral muscle invasion are less commonly seen (Table 2).

MRI features' correlation with molecular markers revealed that there was no significant correlation between the molecular subtype of the breast cancer and the mean age of patients, clinical presentation, parity and menstrual status. The histological type, grading and immunohistochemical markers were also not

Table 1 Distribution of the studied cases according to MRI features of the mass lesions

MRI features of mass lesions	Total ($n=71$)		Mass ($n=63$)		Mass and non-mass ($n=8$)	
	No	%	No	%	No	%
Size (cm)						
< 2	15	21.1	15	23.8	0	0.0
≥ 2	56	78.9	56	76.2	8	100.0
Shape						
Regular	7	9.9	6	9.5	1	12.5
Irregular	64	90.1	57	90.5	7	87.5
Margin						
Circumscribed	5	7.0	5	7.9	0	0.0
Irregular	15	21.1	12	19.0	3	37.5
Spiculated	51	71.8	46	73.0	5	62.5
T2 signal						
Low- intermediate	68	95.8	60	95.2	8	100.0
High signal	3	4.2	3	4.8	0	0.0
Patterns						
Homogeneous	10	14.1	10	15.9	0	0.0
Heterogeneous	51	71.8	44	69.8	7	87.5
Rim enhancement	10	14.1	9	14.3	1	12.5

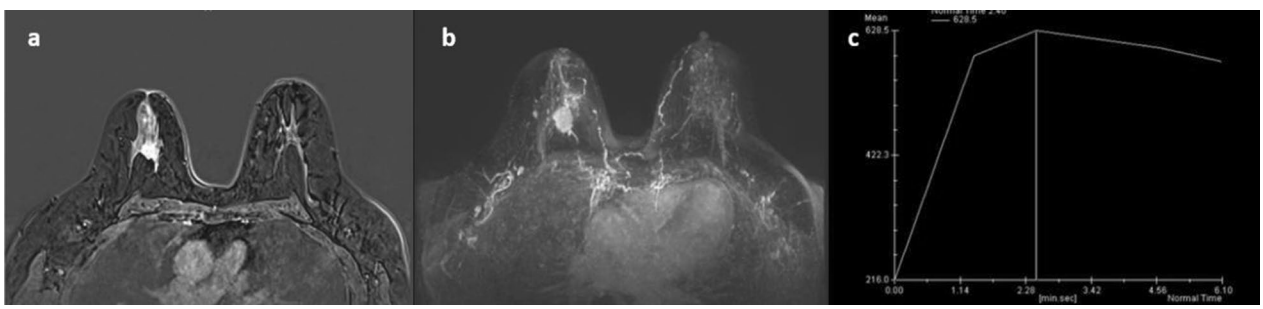

Fig. 2 Rt. Breast pathologically proven invasive ductal carcinoma, NOS, grade III and luminal A type. ITGB 1 FC = 0.01. **a** T1 fat-suppression post-contrast subtracted images, **b** MIP images show an irregular, spiculated outlined soft tissue intensity focal mass lesion, seen at the mid-mammary region, and 12 o'clock area of the Rt. breast, about 37 mm from the nipple, measuring about 24 × 19 × 21 mm, associated with anterior linear anterior intra- ductal extension. It displays intense heterogeneous enhancement at dynamic post-contrast study. **c** Type III-time signal intensity curve. Minimal Rt. sided nippleretraction is seen. Normal MRI appearance of the left breast

Table 2 Distribution of the studied cases according to different MRI features ($n=80$)

MRI features	No	%
Kinetic curve		
Plateau	30	37.5
Washout	50	62.5
Lymph nodes		
No	16	20.0
Yes	64	80.0
ADC value		
Min.–Max	0.88–1.10	
Mean ± SD	0.05 ± 0.96	
Median (IQR)	0.96 (0.93–0.99)	
Associated features		
No	32	40.0
Yes	48	60.0
Skin thickening	24	50.0
Nipple retraction	7	14.6
Perilesional edema	28	58.3
Pectoral muscle invasion	4	8.3

significantly correlated with molecular subtype (Table 3). Also, there was no significant correlation between the molecular subtypes of the breast cancer and the distribution of the lesion. However, it was significantly correlated with the type of the enhancing lesions. Mass lesions were frequently diagnosed with HER2-negative cancers. It was diagnosed in 91.9% of luminal A cancers (Fig. 3), 73.7% in luminal B HER2-negative cancers and 87% of triple-negative ones. However, 50% of HER2-positive cancers presented with non-mass enhancement (Table 4).

The mass lesions showed that there was no significant correlation between the molecular subtype of the breast cancer and the margin of the mass lesions. However, it was significantly correlated with size, shape and pattern of enhancement of the lesion (Table 5). It also revealed no significant correlation between the molecular subtype of the breast cancer and the pattern sand distribution of the non-mass enhancement (Fig. 4). The T2WIs signal, lymph nodes involvement and type of kinetic curve were also not significantly correlated with the molecular subtypes. However, ADC values and perilesional edema were significantly correlated with the molecular subtypes. It was most common seen in patients with luminal B HER2-positive and HER2-amplified subtypes (Table 6).

Regarding type of the lesion, 50% of HER2-+ve cancers showed non-mass enhancement, while most of HER2-−ve lesion showed mass lesions. Molecular markers were also significantly correlated with size, shape, and pattern of enhancement. Most of the cases showed heterogeneous enhancement. On the other hand, 100% of Her 2-enriched and 50% of triple-negative lesion showed ring enhancement (Fig. 5). Higher ADC values were seen in triple-negative and HER2-enriched lesions. Perilesional edema was most common seen in the patients with HER2-+ve lesions (Table 7, Fig.6).

The epigenetic marker linc-ITGB1 was overexpressed by 4.85-fold in breast cancer cases compared to benign controls (Table 8). However, there was no significant correlation between its expression level and the MRI features or molecular subtypes ($p=0.948$) (Table 9).

There was no significant correlation between the average gene expression FC of ITGB1 and mean age of patients, clinical presentation, parity and menstrual status. The histological type, grading and molecular markers were also not significantly correlated with ITGB1 levels (Table 10). As well as there was no significant correlation between the average gene expression FC of ITGB1 and the distribution and lesion and pattern of enhancement (Table 11).

Discussion

Breast cancer is a complex disease with a wide range of clinical behavior, histologic subtypes, therapeutic options, and outcomes [1]. According to the American Joint Committee on Cancer's TNM staging classification, the size of the tumor, histological grade, lymph node involvement, local invasion, and distant metastases are all traditional therapeutic criteria [4].

Patients with the same stage of cancer and similar histological features might have wildly divergent clinical outcomes and prognoses. New molecular subtypes have emerged because of the advances in gene expression analysis using DNA microarray technology: luminal A, luminal B, HER2-enriched, and basal-like. Immunohistochemical staining is reliable to differentiate between these types [1, 2].

The current study included 115 female patients. Eighty patients were pathologically proven to have malignant breast lesions with mean age of 52.85 ± 8.87 (range 37–77). Thirty-five were controls for relative gene expression assessment. Fifty-seven percent of cases were postmenopausal, and seventy-seven percent were multiparous. Ninety-one are presented with different symptoms as breast lump, mastalgia, and nipple discharge. There was no significant correlation between patient's age, parity, menstrual status or the clinical picture and the molecular subtypes or Linc-ITGB1 FC in agreement with the study by Öztürk et al. in which the same results were reported [1]. However, a study carried out by Dogan et al. found that a younger age was significantly associated with the TN subtype [13].

Most of the lesions (93.8%) were pathologically proven to be invasive ductal carcinoma (IDC-NOS), grade II

Table 3 MRI features correlation with molecular markers

	Molecular markers										Test of Sig	*p*
	Luminal A (*n* = 37)		Luminal B HER2-negative (*n* = 19)		Luminal B HER2-positive (*n* = 12)		HER2-amplified (*n* = 4)		Triple-negative (*n* = 8)			
	No	%	No	%	No	%	No	%	No	%		
Age (years)												
< 50	18	48.6	8	42.1	6	50.0	1	25.0	1	12.5	$\chi^2 = 4.195$	$^{MC}p = 0.395$
≥ 50	19	51.4	11	57.9	6	50.0	3	75.0	7	87.5		
Min.–Max	38.0–66.0		43.0–70.0		37.0–77.0		46.0–68.0		47.0–75.0		$F = 1.879$	0.123
Mean ± SD	50.41 ± 7.21		53.21 ± 8.06		54.92 ± 12.89		57.0 ± 9.13		58.13 ± 8.71			
Median	50.0		52.0		51.50		57.0		56.0			
Menstrual status												
Premenopausal	18	48.6	8	42.1	6	50.0	1	25.0	1	12.5	$\chi^2 = 4.195$	$^{MC}p = 0.395$
Postmenopausal	19	51.4	11	57.9	6	50.0	3	75.0	7	87.5		
Clinical presentation												
Asymptomatic	6	16.2	0	0.0	1	8.3	0	0.0	0	0.0	$\chi^2 = 4.105$	$^{MC}p = 0.288$
Symptomatic	31	83.8	19	100.0	11	91.7	4	100.0	8	100.0		
Parity												
Nullipara	6	16.2	8	42.1	2	16.7	1	25.0	1	12.5	$\chi^2 = 5.239$	$^{MC}p = 0.233$
Multipara	31	83.8	11	57.9	10	83.3	3	75.0	7	87.5		
Histological type												
IDC	34	91.9	19	100.0	10	83.3	4	100.0	8	100.0	$\chi^2 = 12.125$	$^{MC}p = 0.625$
ILC	2	5.4	0	0.0	1	8.3	0	0.0	0	0.0		
DCIS	0	0.0	0	0.0	1	8.3	0	0.0	0	0.0		
Mucinous	1	2.7	0	0.0	0	0.0	0	0.0	0	0.0		
Grading of IDC												
I	0	0.0	1	5.3	0	0.0	0	0.0	0	0.0	$\chi^2 = 10.044$	$^{MC}p = 0.265$
II	12	35.3	5	26.3	2	20.0	0	0.0	0	0.0		
III	22	64.7	13	68.4	8	80.0	4	100.0	8	100.0		

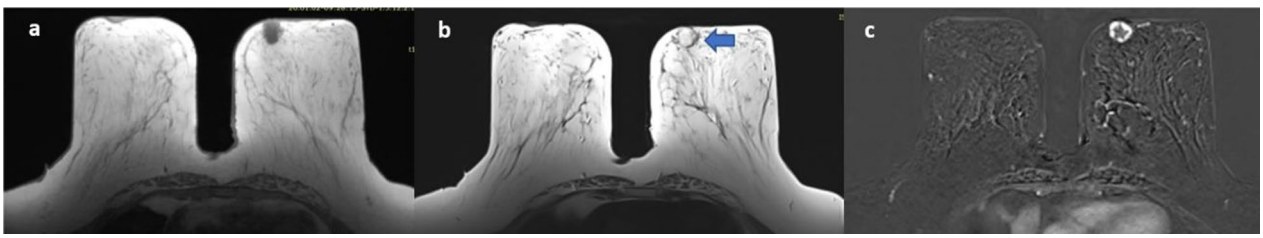

Fig. 3 A 58-year-old patient with Lt. breast mass pathologically proven to be mucinous mammary adenocarcinoma. Immunohistochemical markers in keeping with luminal A type. ITGB Fc = 0.05**a** MRI TIWIs hypo-intense rounded mass lesion with circumscribed margin. Itmeasures 2.1 × 2 cm. **b** in T2 WIs the lesion displays hyperintense signal (arrow). **c** T1 fat-suppression post-contrast subtracted image displays a left mass lesion with ring enhancement. Normal MRI appearance of the right breast

in 25.3% and III in 74.7% of the IDC lesions. The others include mucinous carcinoma (1.3%), invasive lobular carcinoma (3.8%), and ductal carcinoma in situ (1.3%). There was no significant correlation between the tumor pathological type and either the molecular subtypes or the Linc-ITGB1 levels in agreement with Nascimento et al. who reported that IDC-NOS constituting about 40–75% of all invasive breast cancer, mucinous carcinoma responsible for 2% and ILC representing 5% of all newly diagnosed cases [14].

Regarding the molecular subtypes, most of the lesions were of luminal type. Luminal A subtype encountered

Table 4 Relation between the molecular markers and the type of the enhancing lesions and the distribution of the lesion in MRI study ($n=80$)

	Molecular markers										Test of Sig	*p*
	Luminal A ($n=37$)		Luminal B HER2-negative ($n=19$)		Luminal B HER2-positive ($n=12$)		HER2-amplified ($n=4$)		Triple-negative ($n=8$)			
	No	%	No	%	No	%	No	%	No	%		
Distribution of the lesion												
Single	26	70.3	10	52.6	3	25.0	1	25.0	4	50.0	$\chi^2=12.762$	$^{MC}p=0.076$
Multifocal	5	13.5	7	36.8	6	50.0	2	50.0	3	37.5		
Multicentric	6	16.2	2	10.5	3	25.0	1	25.0	1	12.5		
MRI lesion type												
Mass	34	91.9	14	73.7	6	50.0	2	50.0	7	87.5	$\chi^2=14.826$*	$^{MC}p=0.021$*
Non-mass	2	5.4	2	10.5	4	33.3	1	25.0	0	0.0		
Mass + Non-mass	1	2.7	3	15.8	2	16.7	1	25.0	1	12.5		

Table 5 Relation between the molecular markers and the MRI features of mass lesions ($n=80$)

	Molecular markers										Test of Sig	*p*
	Luminal A ($n=37$)		Luminal B HER2-negative ($n=19$)		Luminal B HER2-positive ($n=12$)		HER2-amplified ($n=4$)		Triple-negative ($n=8$)			
	No	%	No	%	No	%	No	%	No	%		
Mass	($n=35$)		($n=17$)		($n=8$)		($n=3$)					
Size (cm)												
<2	14	40.0	0	0.0	1	12.5	0	0.0	0	0.0	$\chi^2=14.044$*	$^{MC}p=0.003$*
≥ 2	21	60.0	17	100.0	7	87.5	3	100.0	8	100.0		
Shape												
Regular	1	2.9	1	5.9	1	12.5	2	66.7	2	25.0	$\chi^2=11.166$*	$^{MC}p=0.009$*
Irregular	34	97.1	16	94.1	7	87.5	1	33.3	6	75.0		
Margin												
Circumscribed	1	2.9	1	5.9	0	0.0	1	33.3	2	25.0	$\chi^2=7.295$	$^{MC}p=0.072$
Not Circumscribed	34	97.1	16	94.1	8	100.0	2	66.7	6	75.0		
Patterns												
Homogenous	7	20.0	1	5.9	2	25.0	0	0.0	0	0.0	$\chi^2=23.638$*	$^{MC}p<0.001$*
Heterogeneous	27	77.1	15	88.2	5	62.5	0	0.0	4	50.0		
Rim enhancement	1	2.9	1	5.9	1	12.5	3	100.0	4	50.0		

in 37 lesions (46.3%). Luminal B HER2 −ve diagnosed in 19 lesions (23.8%) and Luminal B HER2 +ve in 12 lesions (15%). Only 4 lesions (5%) diagnosed as HER2-amplified subtype and 8 lesions (10%) as triple-negative subtype. This was in concordance with Bae et al. in which 181 lesions (64.2%) were classified as luminal A tumors, 30 (10.6%) as luminal B tumors, 22 (7.8%) as HER2−enriched tumors, and 49 (17.4%) as triple-negative tumors [3]. Pandit et al. reported similar results [15]. There was no significant correlation between the molecular subtypes and the Linc-ITGB1 levels.

MRI interpretation included both morphological and kinetic features. The morphological analysis included the size, shape, margin, and pattern of enhancement of the mass lesion. Regarding the non-mass pattern of enhancement, the distribution and pattern of enhancement were evaluated. T2 WIs signal intensity, kinetic curve pattern, lymph node involvement, peri-pectoral edema and skin

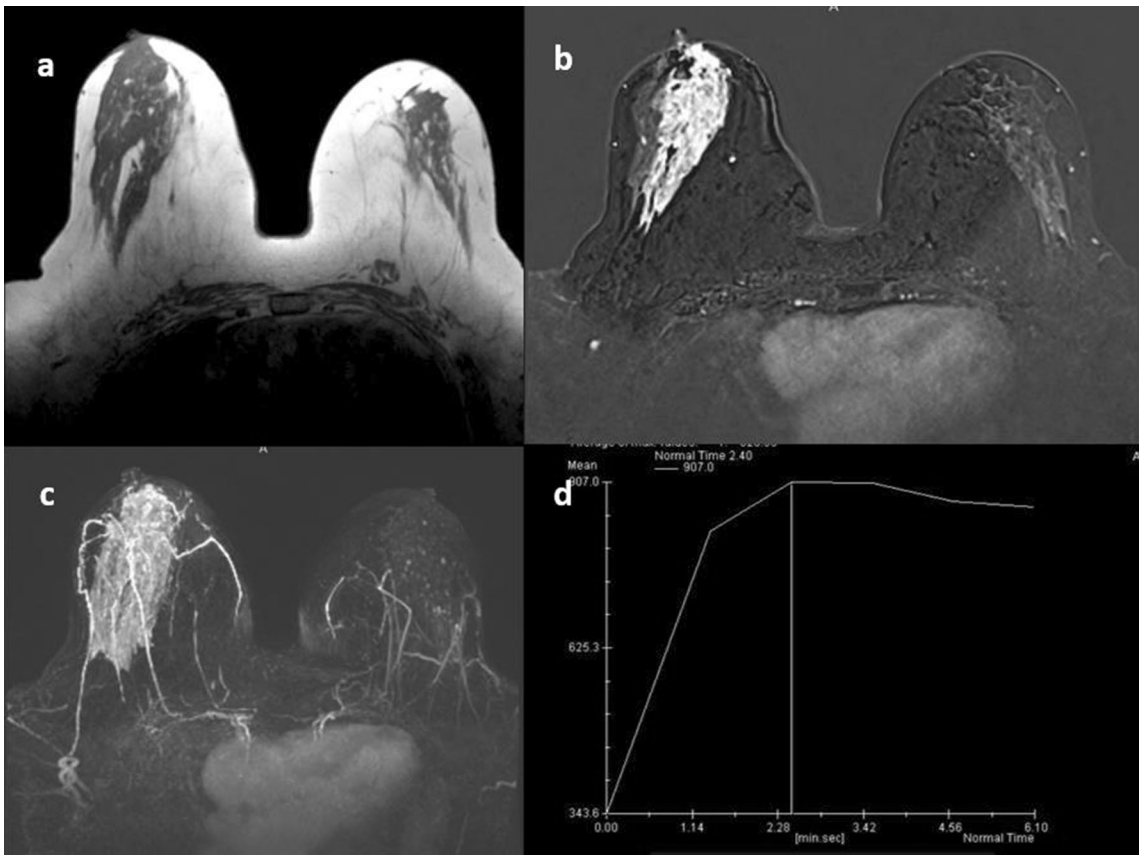

Fig. 4 A 53-year-old patient presented with Rt. breast nipple discharge. Pathological and immunohistochemical assessment revealed a ductal in situ mammary carcinoma and luminal B type (HER2 + ve). ITGB1FC = 2.89. **a** MRI T2WIs **b** T1 fat-suppression post-contrast subtracted image **c** Maximum intensity projection (MIP) image shows a large regional area of non-mass enhancement at the lower-outer quadrant right breast extending to the retro- areolar region showing clumped pattern of internal enhancement **d** Type II time intensity curve. Normal MRI appearance of the left breast

thickening were also evaluated in accordance with the ACR BI-RADS 5th edition Lexicon (2013).

The molecular markers were significantly correlated with the size of the mass lesions ($p = 0.003$). Most of the lesions of triple-negative, HER2-amplified and luminal B subtypes were larger than two centimeters. Sixty percent of the luminal A subtype cases showed mass lesions larger than two centimeters. Dogan et al. found that the mean size of the lesion was larger in the cases with HER2 +ve compared to the luminal A cancers [3]. Li et al., also reported that more aggressive cancers are likely to be larger in size except for mucinous carcinoma [16, 17].

Shape of the lesions in MRI study was significantly correlated with the molecular subtypes ($p = 0.009$). Most of the lesions of luminal A (97%) and luminal B (94%) subtypes show irregular shape and non-circumscribed margins. Only one case of mucinous carcinoma diagnosed as luminal A subtype showed rounded shape and circumscribed margin. Lesions with regular shape and circumscribed margins were seen in 25% of triple-negative cancers and 66.7% of HER 2-amplified cancer showed regular shape.

Dogan et al. reported that spiculated mass margin was significantly associated with luminal A breast cancer (45.2%) and irregular shape was significantly more common in luminal A (86.3%) and luminal B lesions (95.1%) ($p < 0.001$) [13]. On the other hand, Moffa et al. found that 41.7% of TNBC and 86.4% of non-TNBC had irregular shape ($p = 0.005$); 58.3% of TNBC showed circumscribed margins, compared to 9.1% of non-TNBC masses ($p = 0.001$) [18].

DCE-MRI imaging is a noninvasive method for determination of the molecular subtypes. This method can support comprehensive evaluation of heterogeneity of the lesions and predict the prognosis in advance [19]. Regarding the type of enhancement in the current study, it was significantly correlated with the molecular subtypes ($p = 0.021$).

Table 6 Relation between the molecular markers and the MRI features ($n=80$)

	Molecular markers										Test of Sig	*p*
	Luminal A ($n=37$)		Luminal B HER2-negative ($n=19$)		Luminal B HER2-positive ($n=12$)		HER2-amplified ($n=4$)		Triple-negative ($n=8$)			
	No	%	No	%	No	%	No	%	No	%		
Non-mass	($n=3$)		($n=5$)		($n=6$)		($n=2$)		($n=1$)			
Distribution												
Focal	0	0.0	2	40.0	0	0.0	0	0.0	0	0.0	$\chi^2=12.502$	$^{MC}p=0.438$
Linear	0	0.0	1	20.0	1	16.7	1	50.0	0	0.0		
Segmental	3	100.0	2	40.0	4	66.7	0	0.0	1	100.0		
Regional	0	0.0	0	0.0	1	16.7	1	50.0	0	0.0		
Patterns												
Homogenous	0	0.0	2	40.0	0	0.0	0	0.0	0	0.0	$\chi^2=11.883$	$^{MC}p=0.055$
Clumped	3	100.0	3	60.0	6	100.0	2	100.0	0	0.0		
Clustered ring	0	0.0	0	0.0	0	0.0	0	0.0	1	100.0		
T2 signal												
Low-intermediate	36	97.3	19	100.0	12	100.0	4	100.0	6	75.0	$\chi^2=6.558$	$^{MC}p=0.086$
High signal	1	2.7	0	0.0	0	0.0	0	0.0	2	25.0		
Kinetic curve												
Plateau	14	37.8	6	31.6	6	50.0	2	50.0	2	25.0	$\chi^2=2.014$	$^{MC}p=0.760$
Washout	23	62.2	13	68.4	6	50.0	2	50.0	6	75.0		
Lymph nodes												
No	10	27.0	2	10.5	2	16.7	1	25.0	1	12.5	$\chi^2=2.590$	$^{MC}p=0.641$
Yes	27	73.0	17	89.5	10	83.3	3	75.0	7	87.5		
ADC value												
Min.–Max	0.88–1.10		0.88–0.98		0.88–1.04		0.98–1.02		0.96–1.03		$F=10.242$*	<0.001*
Mean ± SD	0.98 ± 0.04		0.92 ± 0.03		0.94 ± 0.04		1.0 ± 0 .02		0.99 ± 0.02			
Median	0.98		0.92		0.94		1.0		0.99			
Associated features												
No	22	59.5	4	21.1	3	25.0	0	0.0	3	37.5	$\chi^2=11.832$*	$^{MC}p=0.013$*
Yes	15	40.5	15	78.9	9	75.0	4	100.0	5	62.5		
Skin thickening	8	53.3	8	53.3	2	22.2	2	50.0	4	80.0	$\chi^2=4.617$	$^{MC}p=0.321$
Nipple retraction	4	26.7	1	6.7	2	22.2	0	0.0	0	0.0	$\chi^2=3.450$	$^{MC}p=0.485$
Perilesional edema	5	33.3	9	60.0	9	100.0	3	75.0	2	40.0	$\chi^2=12.037$*	$^{MC}p=0.009$*
Pectoral muscle invasion	1	6.7	1	6.7	1	11.1	1	25.0	0	0.0	$\chi^2=2.556$	$^{MC}p=0.745$

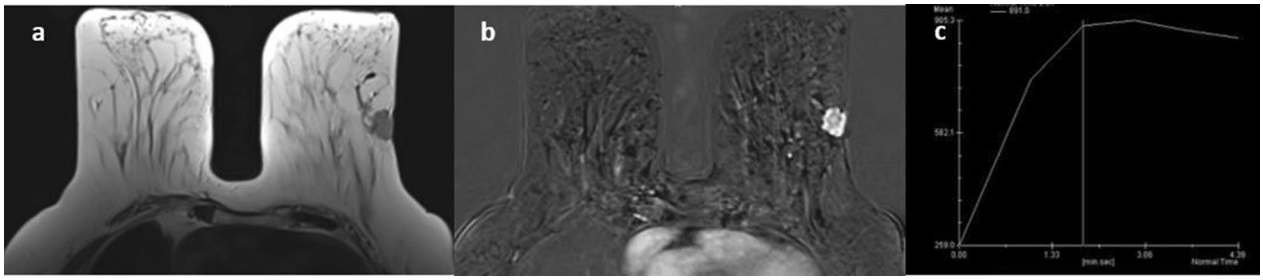

Fig. 5 A 65-year-old patient presented with left breast lump, pathologically proven to be invasive ductal carcinoma, NOS, grade III and triple-negative type. ITGB1 FC = 10.41 **a** MRI T2WIs iso-intense rounded mass lesion with irregular margin. **b** T1 fat-suppression post-contrast subtracted image displays a left subcutaneous mass lesion with ring enhancement. Possible skin invasion is seen. **c** Type II-time signal intensity curve. Normal MRI appearance of the right breast. The imaging features in keeping with triple-negative cancer are rim post-contrast enhancement and skin invasion

Table 7 The molecular markers statistically significant correlations with MRI features

	Molecular markers										**Test of Sig**	***p***
	Luminal A (*n* = 37)		**Luminal B HER2-negative (*n* = 19)**		**Luminal B HER2-positive (*n* = 12)**		**HER2-amplified (*n* = 4)**		**Triple-negative (*n* = 8)**			
	No	**%**	**No**	**%**	**No**	**%**	**No**	**%**	**No**	**%**		
MRI lesion type												
Mass	34	91.9	14	73.7	6	50.0	2	50.0	7	87.5	$\chi^2 = 14.826$*	$^{MC}p = 0.021$*
Non-mass	2	5.4	2	10.5	4	33.3	1	25.0	0	0.0		
Mass + Non-mass	1	2.7	3	15.8	2	16.7	1	25.0	1	12.5		
Mass	(n = 35)		(n = 17)		(n = 8)		(n = 3)					
Size (cm)												
< 2	14	40.0	0	0.0	1	12.5	0	0.0	0	0.0	$\chi^2 = 14.044$*	$^{MC}p = 0.003$*
≥ 2	21	60.0	17	100.0	7	87.5	3	100.0	8	100.0		
Shape												
Regular	1	2.9	1	5.9	1	12.5	2	66.7	2	25.0	$\chi^2 = 11.166$*	$^{MC}p = 0.009$*
Irregular	34	97.1	16	94.1	7	87.5	1	33.3	6	75.0		
Patterns												
Homogenous	7	20.0	1	5.9	2	25.0	0	0.0	0	0.0	$\chi^2 = 23.638$*	$^{MC}p < 0.001$*
Heterogeneous	27	77.1	15	88.2	5	62.5	0	0.0	4	50.0		
Rim enhancement	1	2.9	1	5.9	1	12.5	3	100.0	4	50.0		
ADC value												
Min.–Max	0.88–1.10		0.88–0.98		0.88–1.04		0.98–1.02		0.96–1.03		$F = 10.242$*	< 0.001*
Mean ± SD	0.98 ± 0.04		0.92 ± 0.03		0.94 ± 0.04		1.0 ± 0 .02		0.99 ± 0.02			
Median	0.98		0.92		0.94		1.0		0.99			
Associated features												
Perilesional edema	5	33.3	9	60.0	9	100.0	3	75.0	2	40.0	$\chi^2 = 12.037$*	$^{MC}p = 0.009$*

The non-mass enhancement pattern was found in 11.3% of all cases. In some patients (10%), the mass lesion was associated with non-mass enhancement. However, majority of the cases (78.8%) showed mass pattern of enhancement. Non-mass enhancement was more frequently seen with HER2-positive lesions. It was detected in 50% of the Luminal B HER2-positive and HER2-enriched patients. Most of the non-mass enhancement showed segmental distribution and clumped pattern with no significant correlation with the different molecular subtypes, which is in concordance with a study by Dogan et al. who reported that there were no significant differences in distribution and internal enhancement pattern of the non-mass lesion,

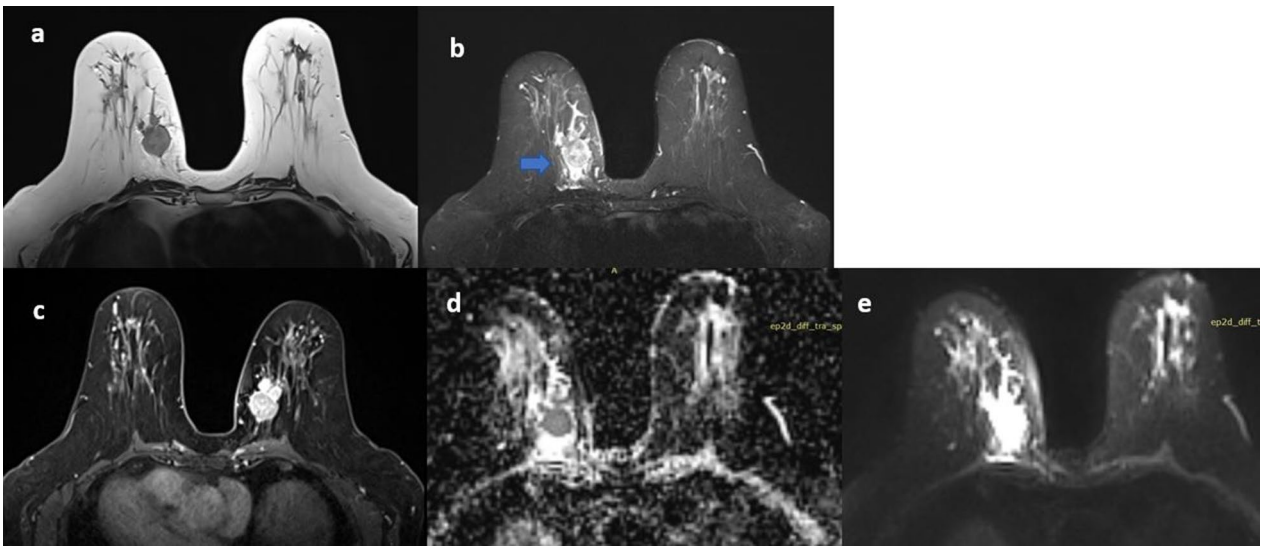

Fig. 6 A 68-year-old patient presented for annual screening. Rt. Breast mass pathologically proven to be invasive ductal carcinoma, NOS, grade III and HER 2-enriched type. ITGB 1 Fc = 8.5. **a** MRI T2WIs hypointense regular mass lesion with circumscribed margin seen at 3 O'clock positions of the Rt. Breast, with 2 anteriorly located inseparable peri-lesional satellites, the overall process measuring about (39 × 27.5 × 29 mm, about 68 mm from the nipple). **b** MRI T2 WIs fat-suppressed image shows mild perilesional interstitial edema (arrow) and **c** T1 fat-suppression post-contrast subtracted image displays a right mass lesion with ring enhancement. **d** DWI shows restricted diffusion. **e** Low ADC values (ADC value = 1.0×10^{-3} s/mm^2) are seen. Normal MRI appearance of the left breast

Table 8 Comparison between the two studied groups according to gene expression fold change (FC)

FC	Cases ($n=80$)	Control ($n=35$)	*U*	*p*
Min.–Max	0.01–4299.64	1.0–1.0	700.0*	< 0.001*
Mean ± SD	96.11 ± 510.78	1.0 ± 0.0		
Median (IQR)	4.85 (0.92–11.2)	1.0		

and time-signal intensity curve pattern among breast cancer subtypes [13].

MR imaging is significantly more likely to help to detect multicentric or multifocal disease and lymph node involvement, especially in luminal B and HER2 molecular subtype breast cancers [20]. A study was carried out by Vilar and German et al. reported that non-mass enhancement was more present in HER2-enriched tumors than in other subtypes and the majority of triple-negative breast cancers (94.1%) were of mass-like enhancement [21]. It was also found that the multicentric lesions are more frequently detected in HER-2-enriched subtype [21], which is consistent with this study in which multifocality and multicentricity were more frequently detected in HER2-positive cases (75%). On the other hand, most of luminal and triple-negative lesions were unifocal. Unifocal lesions were detected in 70.3% of luminal A cancers, 52.6% of luminal B HER2-negative cancers and 50% of triple-negative cancers.

Table 9 Correlation between epigenetic marker expression and molecular subtypes

	Immune histochemical markers										Test of Sig	*p*
	Luminal A ($n=37$)		Luminal B HER2-negative ($n=19$)		Luminal B HER2-positive ($n=12$)		HER2-amplified ($n=4$)		Triple-negative ($n=8$)			
	No	%	No	%	No	%	No	%	No	%		
Epigenetic markers (ITGB1–FC)												
Min.–Max	0.01–1332.6		0.01–4299.6		0.02–42.52		0.14–8.51		0.08–31.34		H = 0.725	0.948
Mean ± SD	269.1 ± 80.42		983.9 ± 237.7		13.86 ± 9.95		4.27 ± 4.88		10.35 ± 7.24			
Median	5.10		2.89		2.82		5.43		2.95			

Table 10 Relation between the epigenetic marker (Linc-ITGB1) and the clinicopathological parameters ($n=80$)

	N	Epigenetic marker (Linc-ITGB1) Median (IQR)	Test of sig	*p*
Age (years)				
< 50	34	6.0 (1.32–18.90)	$U=673.0$	0.289
≥ 50	46	2.81 (0.82–10.41)		
Menstrual status				
Premenopausal	34	6.0 (1.32–18.90)	$U=673.0$	0.289
Postmenopausal	46	2.81 (0.82–10.41)		
Clinical presentation				
Asymptomatic	7	4.96 (3.81–10.55)	$U=233.0$	0.702
Symptomatic	73	3.66 (0.93–10.85)		
Parity				
Nullipara	18	2.82 (0.93–8.0)	$U=517.0$	0.637
Multipara	62	4.88 (1.07–15.56)		
Histological type				
IDC	75	4.89 (1.13–11.05)	$U=99.0$	0.750
ILC	3	2.75 (1.41–12.61)		
DCIS	1#	–		
Mucinous	1#	–		
Grading of IDC				
II	19	6.68 (0.87–13.17)	$U=513.0$	0.817
III	55	4.33 (1.26–11.04)		
Immune histochemical markers				
Luminal	68	4.88 (0.88–16.42)	$U=374.50$	0.652
Non-luminal	12	3.10 (1.38–8.49)		

Table 11 Relation between the epigenetic marker (Linc-ITGB1) and the type and distribution of the lesion in MRI ($n=80$)

	N	Epigenetic marker (Linc-ITGB1) Median (IQR)	Test of sig	*p*
Distribution of the lesion				
Single	44	3.74 (0.81–8.09)	$U=647.50$	0.162
Multiple	36	6.90 (1.87–20.91)		
MRI pattern of enhancement				
Mass	63	5.10 (1.26–10.63)	$H=4.562$	0.102
Non-mass	9	2.89 (2.75–20.11)		
Mass + non-mass	8	1.51 (0.28–2.23)		

The pattern of enhancement of the masses in the current study was significantly correlated with the molecular subtypes ($p<0.001$) detected by Monte Carlo test. Most of luminal breast cancers showed heterogeneous enhancement in post-contrast study. All HER2-positive masses and 50% of triple-negative masses showed peripheral rim of enhancement. This pattern of enhancement is also detected by Azzam et al. in which rim enhancement was predominant in TNBC mass lesions [22]. Rim enhancement was seen most frequently in TN subtype by Dogan, Ozmen et al. [13].

Heterogeneous pattern of enhancement was found in 88.2% of luminal B tumors in the current study, which is consistent with the study by Grimm et al. who detected a statistically significant correlation between luminal B cancers and internal enhancement in which no cases of luminal B cancer demonstrated homogeneous internal enhancement versus a range of 10.9–23.5% for other subtypes [23].

Other MRI features that could differentiate between molecular subtypes of breast cancer included T2 signal intensity. Öztürk et al. explored the relationship between the MRI features and molecular subtypes in which 54% of triple-negative cancers showed high/very high intratumoral T2 signal intensity [1]. In the current study, most of the lesions showed low-to-intermediate signal intensity in T2 WIs. Two cases with triple-negative breast cancer (25%) showed high signal intensity in T2WIs. Only one case of luminal A type showed T2 high signal, which was diagnosed as mucinous adenocarcinoma.

Surov et al. analyzed associations between ADC and hormone receptor status in which ADC was not able to discriminate molecular subtypes of BC and cannot be used as a surrogate marker for disease stage or proliferation activity [12]. Horvat et al. and Wienke et al. detected the same results [11, 24].

In the current study, the mean ADC values ($\times 10^{-3}$ mm^2/s) of the subtypes were as follows: luminal A: 0.98 ± 0.04, luminal B HER2 -ve: 0.92 ± 0.03, luminal B HER2 +ve: 0.94 ± 0.04, Her2− enriched: 1.0 ± 0.02 and triple-negative: 0.99 ± 0.02. There was statistically significant correlation between the ADC values, and the different molecular subtypes with higher ADC values were detected in HER2-enriched and triple-negative subtypes. However, there is still a significant amount of overlap of ADC values among different molecular subtypes.

On the other hand, Allarakha et al. found that lower ADC values were detected in HER2-enriched as compared to HER2 −ve tumors. However, higher ADC values were detected in triple-negative cancers as compared to the HER2-positive and HER2-negative cancers [25].

Many DWI studies have shown that ADC values of breast cancers were lower due to higher cellularity compared with normal or benign breast lesions [26]. Osman et al. found that areas of tumor necrosis showed a significant correlation with increased diffusion and higher ADC values on DWI and was found more frequently in cases of TNBC [27].

A study was carried out by Panzironi et al. to consider peritumoral edema on T2-weighted sequences as a valid additional prognostic tool in the evaluation of breast cancer, since it is associated with biologically aggressive non-luminal breast cancers, characterized by large dimension, high tumor grade, and high Ki-67 values [28]. Dogan et al. also reported that perilesional and prepectoral edema was significantly associated with HER2-positive breast cancer ($p=0.001$) [13]. That agreed with the current study in which there was a significant correlation between the peri-lesional edema and the molecular subtypes ($p=0.009$). HER2-positive cancers were more frequently associated with perilesional edema (100% in luminal B HER2-positive and 75% in HER2-enriched cancers) as compared with HER2-negative cancers.

Skin thickening, nipple retraction and pectoral muscle invasion were assessed with no significant correlation with molecular markers. However, Dogan et al. reported that chest wall or pectoralis muscle invasion was significantly associated with TN breast cancer (1/3, 33.3%) compared with luminal A cancers (0/28, 0%) ($p=0.003$) in non-mass lesions [13]. On the other hand, Lars et al. reported that there was no significant correlation between the pectoral muscle invasion and molecular subtypes [20], which is consistent with the current study. However, this contradiction may be due to the small number of the triple-negative cancers. Further studies with larger sample size may be required.

Ning Liu reported that the presence of axillary lymph nodes is one of the most reliable predictors of overall survival in breast cancer patients, and as such, it has been used in the staging, prognosis, and therapy of invasive breast cancer [29]. This study also found that triple-negative and luminal A breast cancers were more frequently node-negative as compared to luminal B and Her-2-positive cancers. Öztürk et al. reported a significant correlation between HER2-positive breast cancer and the presence of axillary metastatic lymph node [1]. In the current study, 80% of the cases showed axillary lymph node involvement. The luminal A breast cancer showed lower lymph node involvement as compared with luminal B, HER2-enriched and triple-negative cancers, which was against the studies that revealed lower nodal involvement of triple negative. This contradiction may be explained by the large tumor size of triple-negative cases and late stage of lesion discovery in our study.

Yan et al. suggested that linc-ITGB1 promotes breast cancer progression by inducing cell cycle arrest and interrupting the epithelial-to-mesenchymal transition process and reported that the correlation between linc-ITGB1 expression level and clinicopathological features showed that high linc-ITGB1expression was significantly correlated with advanced TNM stage, lymph node metastasis, and high-grade pathological differentiation. However, the level of linc-ITGB1 expression in BC tissues was not associated with the age, tumor size, LNM, ER, PR [5].

Our study was consistent with their research results as the Linc-ITGB1 gene expression FC was not significantly correlated with age, size of lesion, LNM or molecular markers. Our study investigated also the correlation between the Linc-ITGB1 gene expression FC and the dynamic MRI features to investigate the feasibility of using the dynamic MRI study, which is a good predictor for molecular markers and gene expression as well.

In the current study, assessment is done by measuring the expression of linc-ITGB1 by qRT-PCR in BC tissue specimens and matched non-cancerous breast tissue specimens. It was found that mean linc-ITGB1 level in BC tissues was significantly higher than that in normal breast tissues, which is consistent with the study done by Li et al. (6).

Despite the significant correlation between the linc-ITGB1 gene expression FC between BC cases and controls ($p=0.036$, sensitivity = 71.2, specificity = 54.2, PPV = 78.1 and NPV = 45.2), Linc-ITGB1 gene expression FC was not significantly correlated with MRI features which means that we still cannot depend on MRI features to predict the levels of Linc-ITGB1 gene expression.

To appreciate these results, some strength and limitations of our study need to be addressed. In the study, HER2 receptor positivity were present in the subtype luminal-B (HER2-positive) and in the subtype HER2-amplified breast cancers. There was not a single group for all HER2-positive tumors, and this may have influenced our results as compared to other studies. The greatest limitation of this study was that some of the molecular subtypes were not represented by enough cases such as triple-negative and HER2-enriched subtypes. Another limitation is the wide variety of radiological findings rated according to the ACR descriptors. For increasing the statistical analysis precision for similar studies in the future, better representation of all BC molecular subtypes will be requested.

Conclusions

Despite the significant correlation of the Linc-ITGB1 gene expression FC in the malignant lesions as compared with controls, our data could not prove a correlation between MRI features of breast cancer and ITGB1 gene expression. This study can be considered as a preliminary step for applying precision medicine concept in Egypt as it attempted to use multiomics approach via investigating BC patients MRI features (radiomics), molecular features

(genomics and proteomics) and Linc-ITGB1 gene expression (epigenomics) as well. Further studies are needed to investigate the feasibility of combining radiologic features with gene expression and use of artificial intelligence in assessment of MRI-based radiomics to allow a better understanding of tumor behavior and, as a result, to enhance detection and treatment.

Abbreviations

ACR BI-RADS: American college of radiology. Breast imaging reporting and data system.; ADC-MRI: Apparent diffusion coefficient.; AUC: Area under the curve.; BC: Breast cancer.; DCE-MRI: Dynamic contrast-enhanced MRI.; DCIS: Ductal carcinoma in situ; DW-MRI: Diffusion-weighted MRI; ER: Estrogen receptor.; FISH: Fluorescence in situ hybridization; HER2: Human epidermal growth factor receptor 2.; IDC-NOS: Invasive ductal carcinoma-not otherwise specified.; ILC: Invasive lobular carcinoma.; Linc-ITGB1: Long intergenic noncoding RNA-Integrin Subunit Beta 1; LncRNAs: Long non-coding RNAs.; LNM: Lymph node metastasis.; MRI: Magnetic resonance imaging.; NME: Non-mass enhancement.; PR: Progesterone receptor.; Roccurve: Receiver operating characteristic curve.; ROI: Region of interest.; TN: Triple-negative.

Acknowledgements

Not applicable.

Author contributions

AG suggested the research idea, minimized the obstacles to the team of work and had the major role in imaging interpretation. Research data were collected by AS and MA. MR supervised the study with significant contribution to design the methodology, manuscript revision and preparation. HY held the epigenetic assessment of the cases and controls with significant contribution to manuscript revision and preparation. AS was responsible for imaging interpretation, biopsy taking and data analysis. All authors read and approved the final manuscript for submission.

Funding

The cost of the epigenetic marker was covered by the STDF funded project ID: 33941 entitled "The Epigenetic Signature for Egyptian Breast Cancer Patients: Molecular and Clinical Data integration".

Availability of data and materials

The datasets used and analyzed in this study are available from the corresponding author upon reasonable request.

Declarations

Ethics approval and consent to participate

The protocol was reviewed and approved by the Ethics Committee of faculty of medicine, Suez Canal University.

Consent for publication

A written consent for publication was obtained for these cases and approved by the Ethics Committee of faculty of medicine, Suez Canal University. Number of ethical approval (4085#).

Competing interests

The authors declare that they have no competing interests.

Author details

[1]Department of Radiology, Faculty of Medicine, Suez Canal University, Ismailia, Egypt. [2]Medical Genetics Unit, Department of Histology and Cell Biology, Faculty of Medicine, Suez Canal University, Ismailia, Egypt. [3]Department of Oncology, Faculty of Medicine, Suez Canal University, Ismailia, Egypt.

Received: 5 August 2022 Accepted: 21 September 2022
Published online: 28 September 2022

References

1. Öztürk VS, Polat YD, Soyder A, Tanyeri A, Karaman CZ, Taşkın F (2020) The relationship between MRI findings and molecular subtypes in women with breast cancer. Curr Probl Diagn Radiol 49(6):417–421
2. Dai X, Xiang L, Li T, Bai Z (2016) Cancer hallmarks, biomarkers and breast cancer molecular subtypes. J Cancer 7(10):1281–1294
3. Bae MS, Seo M, Kim KG, Park IA, Moon WK (2015) Quantitative MRI morphology of invasive breast cancer: correlation with immunohistochemical biomarkers and subtypes. Acta Radiol 56(3):269–275
4. Chand P, Garg A, Singla V, Rani N (2018) Evaluation of immunohistochemical profile of breast cancer for prognostics and therapeutic use. Niger J Surg 24(2):100–106
5. Yan M, Zhang L, Li G, Xiao S, Dai J, Cen X (2017) Long noncoding RNA linc-ITGB1 promotes cell migration and invasion in human breast cancer. Biotechnol Appl Biochem 64(1):5–13
6. Li WX, Sha RL, Bao JQ, Luan W, Su RL, Sun SR (2017) Expression of long non-coding RNA linc-ITGB1 in breast cancer and its influence on prognosis and survival. Eur Rev Med Pharmacol Sci 21(15):3397–3401
7. Abolghasemi M, Tehrani SS, Yousefi T, Karimian A, Mahmoodpoor A, Ghamari A et al (2020) Critical roles of long noncoding RNAs in breast cancer. J Cell Physiol 235(6):5059–5071
8. Mann RM, Cho N, Moy L (2019) Breast MRI: state of the art. Radiology 292(3):520–536
9. Zhang M, Horvat JV, Bernard-Davila B, Marino MA, Leithner D, Ochoa-Albiztegui RE et al (2019) Multiparametric MRI model with dynamic contrast-enhanced and diffusion-weighted imaging enables breast cancer diagnosis with high accuracy. J Magn Reson Imaging 49(3):864–874
10. Algazzar MAA, Elsayed EEM, Alhanafy AM, Mousa WA (2020) Breast cancer imaging features as a predictor of the hormonal receptor status, HER2neu expression and molecular subtype. Egypt J Radiol Nucl Med 51(1):1–10
11. Horvat JV, Bernard-Davila B, Helbich TH, Zhang M, Morris EA, Thakur SB et al (2019) Diffusion- weighted imaging (DWI) with apparent diffusion coefficient (ADC) mapping as a quantitative imaging biomarker for prediction of immunohistochemical receptor status, proliferation rate, and molecular subtypes of breast cancer. J Magn Reson Imaging 50(3):836–846
12. Surov A, Chang YW, Li L, Martincich L, Partridge SC, Kim JY et al (2019) Apparent diffusion coefficient cannot predict molecular subtype and lymph node metastases in invasive breast cancer: a multicenter analysis. BMC Cancer 19(1):1043
13. Dogan S, Ozmen S, Oz B, Imamoglu H, Kahriman G, Zararsiz G et al (2018) Comparison of different dynamic contrast enhanced-magnetic resonance imaging descriptors and clinical findings among breast cancer subtypes determined based on molecular assessment. Iran J Radiol (**in press**)
14. do Nascimento RG, Otoni KM (2020) Histological and molecular classification of breast cancer: what do we know? Mastology. 30:e20200024
15. Pandit P, Patil R, Palwe V, Gandhe S, Patil R, Nagarkar R (2019) Prevalence of molecular subtypes of breast cancer: a single institutional experience of 2062 patients. Eur J Breast Health. 16(1):39–43
16. Li H, Zhu Y, Burnside ES, Huang E, Drukker K, Hoadley KA et al (2016) Quantitative MRI radiomics in the prediction of molecular classifications of breast cancer subtypes in the TCGA/TCIA data set. NPJ Breast Cancer 2:1–10
17. Kawashima M, Tamaki Y, Nonaka T, Higuchi K, Kimura M, Koida T et al (2002) MR imaging of mucinous carcinoma of the breast. Am J Roentgenol 179:179–183
18 Moffa G, Galati F, Collalunga E, Rizzo V, Kripa E, D'Amati G et al (2020) Can MRI biomarkers predict triple-negative breast cancer? Diagnostics (Basel) 10(12):1090
19. Li W, Yu K, Feng C, Zhao D (2019) Molecular subtypes recognition of breast cancer in dynamic contrast-enhanced breast magnetic resonance imaging phenotypes from radiomics data. Comput Math Methods Med 2019:6978650
20 Grimm LJ, Johnson KS, Marcom PK, Baker JA, Soo MS (2015) Can breast cancer molecular subtype help to select patients for preoperative MR imaging? Radiology 274(2):352–358
21. Navarro Vilar L, Alandete German SP, Medina Garcia R, Blanc Garcia E, Camarasa Lillo N, Vilar SJ (2017) MR imaging findings in molecular subtypes of breast cancer according to BIRADS system. Breast J 23(4):421–428

22. Azzam H, Kamal R, El-Assaly H, Omer L (2020) The value of dynamic contrast-enhanced MRI in the diagnosis and management of triple-negative breast cancer. Egypt J Radiol Nucl Med 51(1):1–6
23. Grimm LJ, Zhang J, Baker JA, Soo MS, Johnson KS, Mazurowski MA (2017) Relationships between MRI breast imaging-reporting and data system (BI-RADS) lexicon descriptors and breast cancer molecular subtypes: internal enhancement is associated with luminal B subtype. Breast J 23(5):579–582
24. Meyer H-J, Wienke A, Surov A (2021) Diffusion-weighted imaging of different breast cancer molecular subtypes: a systematic review and meta-analysis. Breast Care. https://doi.org/10.1159/000514407
25. Allarakha A, Gao Y, Jiang H, Wang PJ (2019) Prediction and prognosis of biologically aggressive breast cancers by the combination of DWI/DCE-MRI and immunohistochemical tumor markers. Discov Med 27(146):7–15
26. Kim SY, Kim EK, Moon HJ, Yoon JH, Koo JS, Kim SG et al (2018) Association among T2 signal intensity, necrosis, ADC and Ki-67 in estrogen receptor-positive and HER2-negative invasive ductal carcinoma. Magn Reson Imaging 54:176–182
27. Osman NM, Chalabi N, Raboh NMA (2014) Triple negative breast cancer: MRI features in comparison to other breast cancer subtypes with correlation to prognostic pathologic factors. Egypt J Radiol Nucl Med 45(4):1309–1316
28. Panzironi G, Moffa G, Galati F, Marzocca F, Rizzo V, Pediconi F (2020) Peritumoral edema as a biomarker of the aggressiveness of breast cancer: results of a retrospective study on a 3 T scanner. Breast Cancer Res Treat 181(1):53–60
29. Liu N, Yang Z, Liu X, Niu Y (2017) Lymph node status in different molecular subtype of breast cancer: triple negative tumours are more likely lymph node negative. Oncotarget 8(33):55534–55543

Publisher's Note